BRITISH ACOUSTICAL SOCIETY

71SC5

British Acoustical Society
Spring Meeting, 5-7 April 1971,
University of Birmingham

VERY LOW FREQUENCY SOUND ATTENUATION MEASUREMENTS

by

R. H. Mellen, W. H. Thorp, L. C. Maples, E. N. Jones, D. G. Browning
Naval Underwater Systems Center, New London Laboratory
U.S.A.

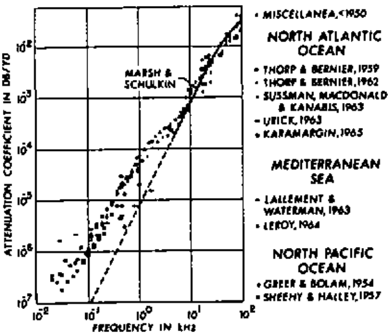

Fig. 1

Measurements of sound propagation in the ocean have established the existence of two distinct regimes of excess attenuation. The first of these has been identified with the M_gSO_4 content of sea water and is indicated by the dashed line of Fig. 1. The other experimental data below 1 kHz show values some ten times higher, and concur in the existence of an anomaly if not in its precise behavior.

Evidently, the low frequency attenuation anomaly has excited the interest of many investigators who have proposed a number of possible explanations (Fig. 2). Many of these have already been fairly well discounted and attention has tended to focus on a second relaxation-absorption as a likely mechanism.

POSSIBLE EXPLANATIONS FOR ATTENUATION ANOMALY

1. SUSPENDED MATTER	DUYKERS, 1967
2. BIOLOGICAL SCATTERING	WESTON, 1966
3. FINITE-AMPLITUDE EFFECTS	MARSH, MELLEN, KONRAD, 1965
4. INHOMOGENEITIES	URICK, 1963
5. EDDY VISCOSITY	SCHULKIN, 1963
6. CHANNEL LEAKAGE	URICK, 1963
7. INTERNAL WAVES	(NO CALCULATIONS)
8. RELAXATION PROCESS (UNKNOWN)	THORP, 1965 URICK, 1966 LE ROY, 1964
9. RELAXATION PROCESS-IONS	HORNE, 1968
10. RELAXATION PROCESS-WATER	BROWNING, THORP, MELLEN, 1968
11. DISSOLVED CO_2	FISHER 1969
12. PLANKTON	DUYKERS 1970

Fig. 2

Figure 3 shows the low frequency attenuation data fitted to a relaxation-absorption curve. The complete analytic expression is given by the α equation where the first term is the $MgSO_4$ relaxation term (f_r = 64 kHz) and the second is the anomalous term (f_r = 1 kHz). The general agreement between continuous wave and explosive measurements is taken as evidence against the finite amplitude explanation.

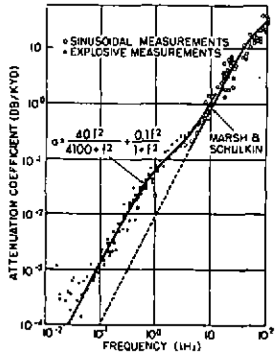

EXPERIMENTAL ATTENUATION COEFFICIENTS

Fig. 3

We have been trying to identify the precise behavior and possibly the cause of the anomaly by carrying out a series of propagation experiments in waters of different temperature and salinity. Figure 4 illustrates our experimental technique. Bodies of water are chosen primarily for their suitability as refraction sound channels so that losses will occur within the water and not at the boundaries. A sound channel is formed by the combined effects of the higher temperature at the surface and the pressure effect at the bottom. The resulting increase in sound speed toward both boundaries causes the sound to be refracted toward the sound speed minimum which is the sound channel axis.

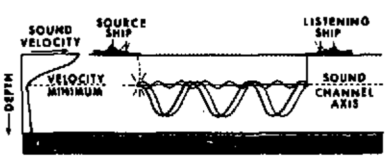

DIAGRAM OF EXPERIMENT

Fig. 4

Explosive charges are detonated on the sound channel axis at various ranges from the listening ship. The acoustic signals are received by means of a hydrophone also located on the axis, and the electrical signal is recorded on magnetic tape for later analysis.

It would seem from the results for the cantilevered triangular plate that it is desirable in such cases to use a minimum number of triangles for greatest accuracy.

4. REFERENCES

1. G. R. COWPER et al. 1968 National Research Council of Canada, Aeronautical Rpt. LR-514. A high precision triangular plate-bending element.

2. V. MASON 1968 J. Sound Vib. 7, 437. Rectangular finite elements for analysis of plate vibrations.

3. P. N. GUSTAFSON et al. 1953 J. Aero. Sci. 20, 331. An experimental study of natural vibrations of cantilevered triangular plates.

	FREQUENCY (Hz.)				
MODE NUMBER					Experimental Results Reference (3)
1	36.54124	36.53947	36.53897	36.53895	34.5
2	138.9636	138.9567	138.9550	138.9528	136.0
3	193.6010	193.5815	193.5754	193.5699	190.0
4	332.7147	332.7060	332.6953	332.6240	325.0
5	453.2197	453.2150	453.0388	452.9050	441.0
6	589.2431	589.1010	589.0678	588.6882	578.0
7	664.0397	663.8512	663.7170	662.9144	
8	798.0966	797.7241	796.9290	796.3389	
9	948.1436	947.2899	946.1370	944.4312	
10	1092.781	1092.583	1091.741	1088.801	

TABLE 1 NATURAL FREQUENCIES OF CANTILEVERED TRIANGULAR PLATE OF ASPECT RATIO 1

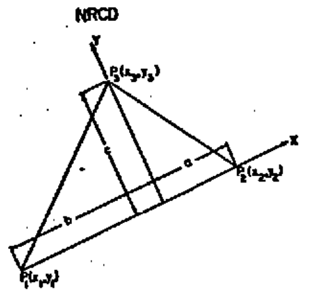

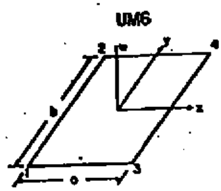

$$w(x,y) = a_1 + a_2 x + a_3 y + a_4 x^2 + a_5 xy + a_6 y^2 + a_7 x^3 + a_8 x^2 y + a_9 xy^2 + a_{10} y^3 + a_{11} x^4 + a_{12} x^3 y + a_{13} x^2 y^2 + a_{14} xy^3 + a_{15} y^4 + a_{16} x^5 + a_{17} x^3 y^2 + a_{18} x^2 y^3 + a_{19} xy^4 + a_{20} y^5$$

$$w(x,y) = a_1 + a_2 x + a_3 y + a_4 x^2 + a_5 xy + a_6 y^2 + a_7 x^3 + a_8 x^2 y + a_9 xy^2 + a_{10} y^3 + a_{11} x^4 + a_{12} x^3 y + a_{13} x^2 y^2 + a_{14} xy^3 + a_{15} y^4 + a_{16} x^5 + a_{17} x^3 y^2 + a_{18} y^3 x^2 + a_{19} y^5 + a_{20}\left(\frac{yb}{2} - \frac{2}{3}\frac{y^3}{b}\right)x^4 + a_{21}\left(\frac{xa}{2} - \frac{2}{3}\frac{x^3}{a}\right)y^4 + a_{22} x^3 y^3 + a_{23}\left(\frac{yb}{2} - \frac{2}{3}\frac{y^3}{b}\right)x^5 + a_{24}\left(\frac{xa}{2} - \frac{2}{3}\frac{x^3}{a}\right)y^5$$

Figure 1. DISPLACEMENT FUNCTIONS FOR THE UM6 AND NRCD ELEMENTS

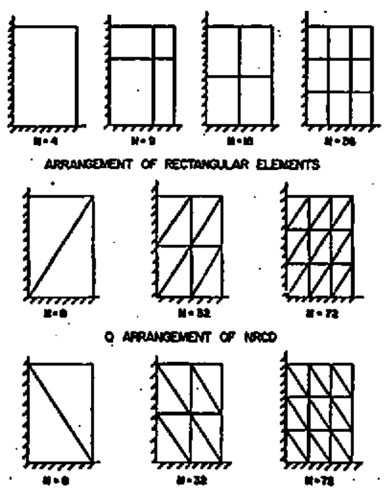

Figure 2. LAYOUT OF FINITE ELEMENTS FOR DYNAMIC ANALYSIS OF THE RECTANGULAR PLATE (NB. only quarter of plate shown)

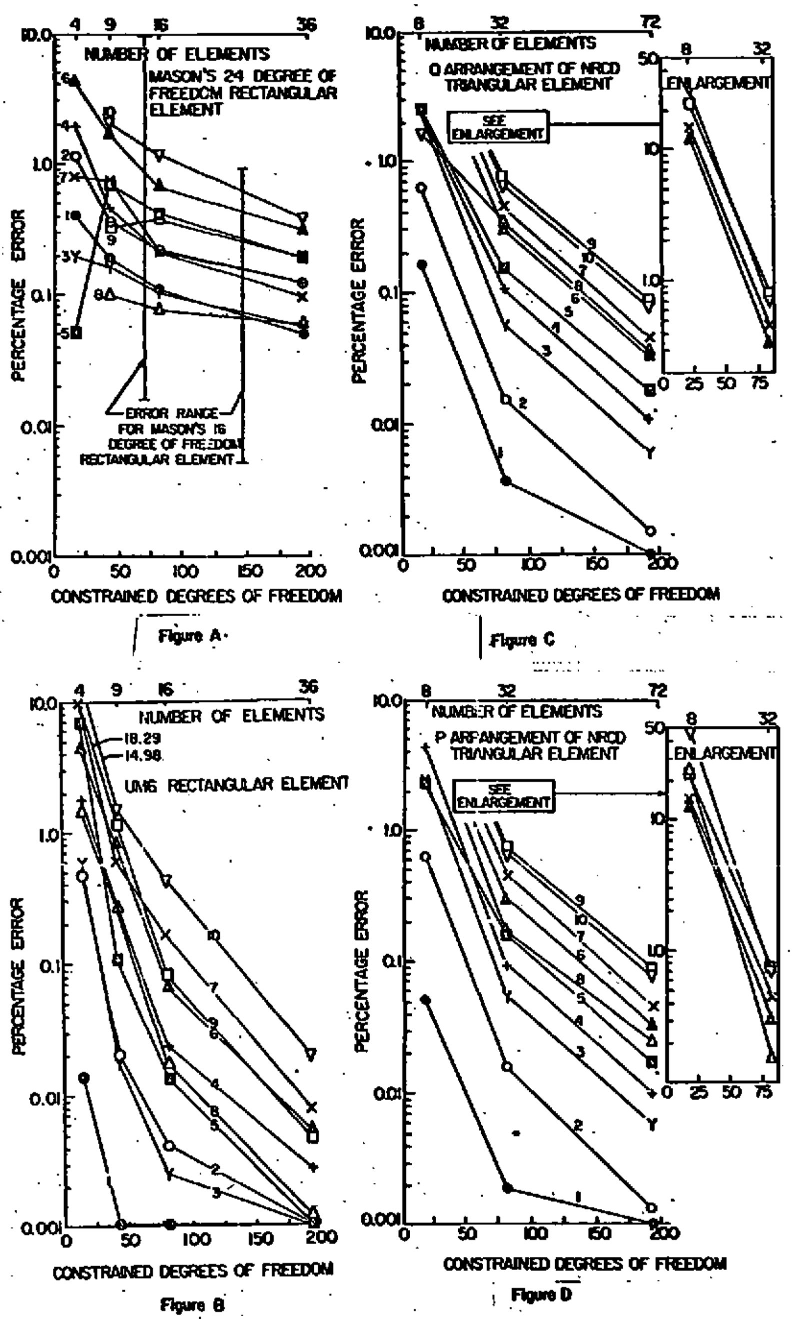

Figure 3. PERCENTAGE ERROR IN THE NATURAL FREQUENCIES OF A 40:27 SIMPLY SUPPORTED PLATE FOR DIFFERENT TRIANGULAR AND RECTANGULAR ELEMENTS.

The recorded signals are analyzed using 1/3-octave filters to determine the peak pressure response at the selected frequencies. The received pressure level is then subtracted from the known source level to obtain the appropriate value of propagation loss as a function of frequency. Figure 5 shows a typical data plot of loss vs. range for the frequency 1410 Hz. From the value of propagation loss 10 log R was subtracted for cylindrical spreading so that the slope of a straight line fit gives the attenuation directly in decibels per unit distance. The intercept at zero range indicates the additional loss due to spherical spreading near the source.

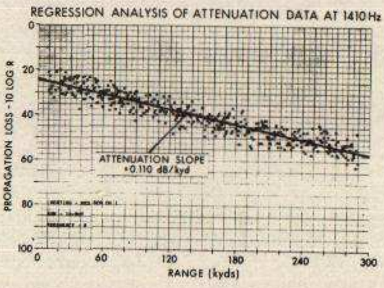

Fig. 5

Figure 6 shows our experimental values of α vs. frequency for the 1969 Red Sea Experiment. The solid line is the Thorp curve of Fig. 2. The fit is seen to be reasonably good except for the slightly higher Red Sea value from 1-10 kHz. A more precise relaxation curve fit to the data in fact gives an apparent relaxation frequency of 1.5 kHz compared to 1 kHz for Thorp.

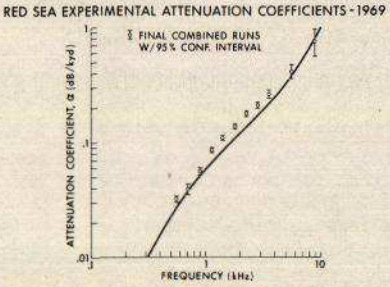

Fig. 6

The relaxation hypothesis, of course, requires an increase in relaxation frequency with temperature. Figure 7

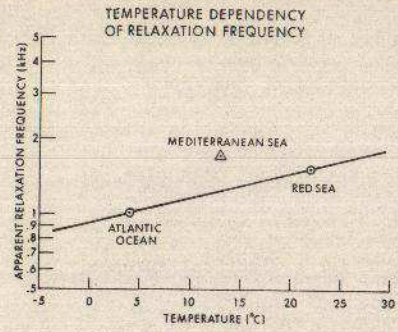

Fig 7.

shows our two relaxation frequencies vs. temperature together with LeRoy's 1.7 kHz value for the Mediterranean. The lack of a uniform trend of the three values is apparent, even though the overall consistency of relaxation-like behavior of the experimental data is still impressive.

The Hudson's Bay results, Fig. 8 , tend to weaken the relaxation hypothesis. (This was a joint U.S./Canadian experiment carried out with Defense Research Establishment Atlantic, Halifax, August 1970.) It is apparent that the values of α are not only considerably in excess of Thorp (solid line) but also do not fit a relaxation curve well at all.

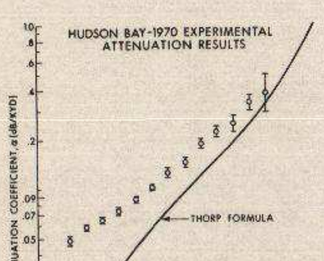

Fig. 8

At this point there are several possible reasons for the apparent dilemma: (1) The data may be subject to systematic error (which can be eliminated with improved analytical methods), (2) The simplified sound channel model may be inadequate (we are presently experimenting with a Fast Fourier Field Program), (3) More than one mechanism may be involved (volume scattering and bottom leakage for example).